

# Chapter 2

## MIMO Wireless Communications

The multiple input multiple output (MIMO) technique provides the higher bit rate and the better reliability in wireless systems. These advantages are achieved by designing appropriate space-time codes that provide diversity improvement, spatial multiplexing gain, or a trade-off between diversity order and spatial multiplexing. This chapter provides an overview on MIMO wireless system concept and its performance. Moreover, the MIMO channel models are discussed.

### 2.1 MIMO System

A multiple input multiple out (MIMO) system with  $M_T$  transmitting antennas and  $M_R$  receiving antennas is shown in Figure 2.1. The input data are transmitted through  $M_T$  antennas after processing on the transmitter side. The processing includes channel coding, modulation, space-time encoding, spatial mapping, and radio frequency (RF) up-conversion. Each antenna transmits a signal through a wireless channel. Accordingly, the  $M_T$  antennas simultaneously operate as an entire transmitter. The radiated signals are represented by a column vector ( $\mathbf{x}$ ) that has  $M_T \times 1$  dimensions. These signals, after passing through the wireless channel, are received by  $M_R$  receiving antennas.

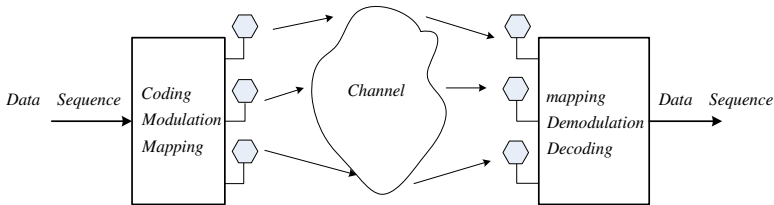


**Fig. 2.1** Block diagram of a MIMO system

## 2.2 MIMO Channel

The impulse response of a linear time-varying communication system between a transmitter and a receiver is used to describe the effects of a linear transmission channel.

### 2.2.1 SISO Channel Model

In the first step, a narrowband system using a single antenna at both the transmitter and the receiver is assumed (single input single out – SISO). The symbol period is assumed to be  $T$ . Moreover, the digital signal in discrete time may be represented by the complex time series  $\{x_k\}$ .

In this case, the transmitted signal is represented by:

$$x(t) = \sum_{m=-\infty}^{\infty} \sqrt{E_s} x_m \delta(t - mT) \quad (2.1)$$

where  $E_s$  is the transmitted symbol energy, assuming that the average energy constellation is normalized to unity. In a linear time-invariant (LTI) system, a function  $h(t)$  as the time-invariant impulse response of the channel can be considered [1]. If the signal  $x(t)$  is transmitted, the received signal  $r(t)$  is given by

$$r(t) = h(t) * x(t) + n(t) \quad (2.2)$$

where  $*$  denotes the convolution product, and  $n(t)$  is the additive noise of the system. Therefore, the input-output relation is represented as:

$$r(t) = \sum_{m=-\infty}^{\infty} \sqrt{E_s} x_m h(t - mT) + n(t) \quad (2.3)$$

One obtains the discrete representation of the received signal by sampling the received signal at the rate of  $T$ , ( $r(kT)$ ) as:

$$r(kT) = \sum_{m=-\infty}^{\infty} \sqrt{E_s} x_m h[(k - m)T] + n(kT) \quad (2.4)$$

$$r[k] = \sum_{m=-\infty}^{\infty} \sqrt{E_s} x_m h[k - m] + n[k]$$

As may be seen, a time-invariant channel can be represented as an LTI system and its sampled representation  $h[k]$ . The extension of this representation to a time-varying channel is completely straightforward [2], [4]. Moreover, there are

different methods to extract the channel impulse response both in narrowband and broadband transmissions [3]. The channel impulse response generally depends on attenuation of the path loss term, shadowing, and multipath fading.

### 2.2.2 MIMO Channel Modeling

In MIMO systems, both the transmitter and receiver have several antennas. A MIMO system with  $M_T$  transmitting antennas and  $M_R$  receiving antennas is shown in Figure 2.2. In this system, the channel between each transmitting-receiving antenna pair can be modeled as a SISO channel. Accordingly, the channel matrix ( $\mathbf{H}$ ) for a MIMO system with  $M_T$  transmitting antennas and  $M_R$  receiving antennas may be obtained. By arranging all inputs and outputs in vectors,  $\mathbf{x}[k] = [x_{1,k}, \dots, x_{M_T,k}]^T$  and  $\mathbf{r}[k] = [r_{1,k}, \dots, r_{M_R,k}]^T$ , the input-output relationship at any given time instant ( $k$ ) is obtained as:

$$\mathbf{r}[k] = \sqrt{E_s} \mathbf{H}[k] \mathbf{x}[k] + \mathbf{n}[k] \quad (2.5)$$

where  $\mathbf{H}[k]$  is defined as the  $M_R \times M_T$  MIMO channel matrix in sampling time  $kT$ , and  $\mathbf{n}[k] = [n_{1,k}, \dots, n_{M_R,k}]^T$  is the sampled noise vector, containing the noise contribution at each receive antenna, such that the noise is white in both time and spatial dimensions as:

$$E\{\mathbf{n}[k]\mathbf{n}[m]\} = \sigma_n^2 \mathbf{I}_{M_R} \delta[k-m] \quad (2.6)$$

where  $\sigma_n^2$  is the Gaussian noise variance and  $\mathbf{I}_{M_R}$  is the identity matrix. By normalizing the transmit symbol energy to unity, the received signal is shown to be:

$$\mathbf{r} = \mathbf{H}\mathbf{x} + \mathbf{n} \quad (2.7)$$

where  $\mathbf{r}$  is the received column vector signal with dimensions of  $M_R \times 1$  composed of the received signal,  $r_j$ ;  $\mathbf{n}$  is an  $M_R \times 1$  column vector composed of the noise components,  $n_j$ ; and,  $\mathbf{H}$  is the  $M_R \times M_T$  channel matrix with  $j$ th component being the channel coefficient,  $h_{j,i}$ . Accordingly, a MIMO system can be represented using the following matrix equation:

$$\begin{bmatrix} r_1 \\ \vdots \\ r_{M_R} \end{bmatrix} = \begin{bmatrix} h_{1,1} & \cdots & h_{1,M_T} \\ \vdots & \ddots & \vdots \\ h_{M_R,1} & \cdots & h_{M_R,M_T} \end{bmatrix} \begin{bmatrix} x_1 \\ \vdots \\ x_{M_T} \end{bmatrix} + \begin{bmatrix} n_1 \\ \vdots \\ n_{M_R} \end{bmatrix} \quad (2.8)$$

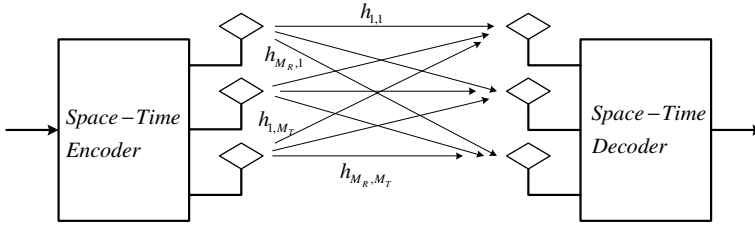


**Fig. 2.2** MIMO channel

■ **Example 2.1:** *Independent and Identically distributed Rayleigh MIMO Channel*

If each individual channel coefficient is a zero-mean complex, circularly symmetric Gaussian variable or, equivalently, a complex variable whose amplitude and phase are Rayleigh and uniformly distributed, respectively, it is called a wide-sense stationary uncorrelated scattering homogeneous (WSSUSH) Rayleigh fading channel [4]. When the antenna spacing on both sides of the link is large enough, the various channel correlations become very small and can be assumed to be equal to zero [2]. The typical antenna spacing for negligible correlation is about  $\lambda/2$ , where  $\lambda$  is the wavelength. Furthermore, if all individual channel coefficients are characterized by the same average power, the channel matrix is represented as  $\mathbf{H}_w$ . This is a random fading matrix with unit variance and circularly symmetric complex Gaussian entries. This channel, which uses the independent and identically distributed (i.i.d.) assumption, is represented by as  $CN(0,1)$ .

## 2.3 MIMO Capacity

The channel capacity is a fundamental limit on the rate of error-free messages that can be transmitted through a communication channel. In this section, the capacity of SISO and MIMO channels under fading are discussed.

### 2.3.1 SISO Capacity

The channel capacity for SISO communication systems over additive white Gaussian noise (AWGN) channels has been extracted by Shannon as:

$$C = B \log_2 \left( 1 + \frac{S}{N} \right) \quad (2.9)$$

where  $C$  is the channel capacity in bit per second,  $B$  is the channel bandwidth in Hz,  $S$  is the transmitted power, and  $N$  is the noise power in the channel bandwidth.

Defining  $\gamma \triangleq S/N$ , the channel capacity for fading channels can be obtained as [5], [6]:

$$C = \int_0^{\infty} B \log_2(1 + \gamma) p_{\gamma}(\gamma) d\gamma \quad (2.10)$$

where  $p_{\gamma}(\gamma)$  is the probability density function of fading channel.

### 2.3.2 MIMO Capacity

MIMO systems with multiple antennas on both the transmitting and receiving sides have been considered. The capacity of MIMO systems can be expressed in bits per second per hertz (bps/Hz) as [4], [7]:

$$C = \max \left\{ \log_2 \det \left( I_{M_R} + \frac{\gamma}{M_T} H R_{ss} H^H \right) \right\} \quad (2.11)$$

$$T_r(R_{ss}) = M_T$$

where  $I_{M_R}$  is the identity matrix,  $H$  is the channel matrix with  $H^H$  being its transpose conjugate,  $R_{ss} = E\{ss^H\}$  is covariance matrix of the transmit signal,  $\gamma$  gives the average signal-to-noise ratio (SNR) per receiver branch, and  $T_r(\cdot)$  represents the trace of a matrix. As can be seen, the channel capacity may be reached by choosing the optimal covariance structure for the transmitted signals. If the channel is unknown on the transmitter side, the transmitted signal can be considered spatially white, e.g.,  $R_{ss} = I_{M_T}$ . Accordingly, the MIMO channel capacity for a sample deterministic realization is given by:

$$C = \log_2 \det \left( I_{M_R} + \frac{\gamma}{M_T} H H^H \right) \quad (2.12)$$

If the eigendecomposition of  $H H^H$  is represented as  $Q \Lambda Q^H$ , where  $Q$  is an  $M_R \times M_R$  matrix satisfying  $Q Q^H = Q^H Q = I_{M_R}$  and  $\Lambda = \text{diag}\{\lambda_1, \lambda_2, \dots, \lambda_{M_R}\}$  with  $\lambda_i \geq 0$ , equation (2.12) can be written as:

$$C = \log_2 \det \left( I_{M_R} + \frac{\gamma}{M_T} Q \Lambda Q^H \right) \quad (2.13)$$

By using the identity of  $\det(I_m + AB) = \det(I_n + BA)$  for  $A_{mn}, B_{nm}$  and using  $QQ^H = Q^H Q = I_{M_R}$ , the capacity relation may be written as:

$$C = \log_2 \det(I_{M_R} + \frac{\gamma}{M_T} \Lambda) \quad (2.14)$$

This relation equivalently may be represented as:

$$C = \sum_{i=1}^r \log_2 (1 + \frac{\gamma}{M_T} \lambda_i) \quad (2.15)$$

where  $r$  is the rank of channel and  $\lambda_i \geq 0$  are the eigenvalues of  $HH^H$  [4].

Equation (2.12) can be also used to obtain the MIMO capacity in the fading channel. Extending equation (2.10) for an MIMO channel, the capacity of the MIMO channel under fading can be represented by:

$$C = E\{\log_2 \det(I_{M_R} + \frac{\gamma}{M_T} HH^H)\} \quad (2.16)$$

where the average is over the distribution of the elements of  $H$ .

In order to provide a clear idea about MIMO capacity, the asymptotic MIMO capacity should be examined. Assuming the spatially white Gaussian channel ( $CN(0,1)$ ) and using the law of large numbers considering large  $M$  ( $M_T = M_R = M$ ) [14], [7] yields:

$$\frac{1}{M} H_W H_W^H \rightarrow I_M \quad M \rightarrow \infty \quad (2.17)$$

where  $H_W$  is the spatially white Gaussian channel. Accordingly, the capacity can be written as:

$$C = M \log_2(1 + \gamma) \quad (2.18)$$

This interesting result shows that the capacity increases linearly with an increasing number of antennas.

The capacity of a single input multiple out (SIMO) system, which is also known as the receiver diversity, can be expressed as [7]:

$$C_{SIMO} = \log_2(1 + \gamma M_R) \quad (2.19)$$

As can be seen, only the logarithmic improvement in capacity with increasing  $M_R$  is achievable in the SIMO system. For a random channel, this relation is valid for both the known channel state information (CSI) at the transmitter and the unknown CSI. This is due to the implementation of a single transmitting antenna. The capacity of the multiple input single output (MISO) channel when no CSI is provided at transmitter is obtained as:

$$C_{SIMO} = \log_2(1 + \gamma) \tag{2.20}$$

The capacity of the MISO system with a known CSI at transmitter is expressed as:

$$C_{MISO} = \log_2(1 + \gamma M_T) \tag{2.21}$$

■ **Example 2.2:** Capacity Estimation for 2X2 MIMO System

The capacity of a 2X2 MIMO system is presented in this example [25]. As shown in Figure 2.3, a MIMO system with polarized matched transmitting and receiving antennas is assumed. The antennas gains are 0 dBm.

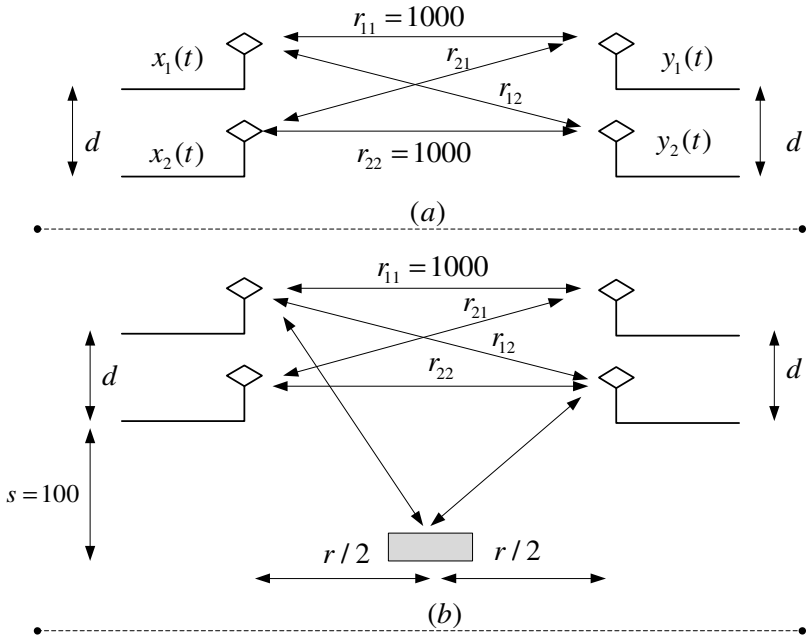


**Fig. 2.3** Capacity estimation for 2X2 MIMO channel: a) without scattering b) with single scattering [25]

The communications system operates at 1.9 GHz with a 200 KHz bandwidth and a transmitting power of 1 mW. The noise temperature is 300 K. The capacity is calculated in the following cases:

**Case I: SISO Capacity**

The received power due to the propagation path loss is a function of frequency operation and is obtained as:

$$P_r = P_t G_t G_r \left( \frac{16\pi^2 d^n}{\lambda^2} \right)$$

where  $P_r, P_t$  are the receiving and transmitting powers;  $G_r, G_t$  are the receiving and transmitting antenna gains;  $d$  is the distance between the transmitter and the receiver;  $n$  is the path loss exponent, which is usually between 2 and 6; and,  $\lambda$  is the free space path length. In this example, it is assumed that  $n = 2$ . Using the above relations and equation (2.20):

$$\begin{aligned} P_r &= 1.58 \times 10^{-13} \text{ W } (-98 \text{ dBm}) \\ N_o &= kT_e B = 8.28 \times 10^{-16} \text{ W } (-120.8 \text{ dBm}) \\ \gamma &= 22.8 \text{ dBm} \\ C_{\text{ISI}} &= \log_2(1 + \gamma) = 7.6 \quad \text{bps / Hz} \end{aligned}$$

**Case II: MIMO Capacity without Scattering**

As illustrated in Figure 2.3(a), by calculating  $\mathbf{H}$  and using equation (2.15):

$$\mathbf{H} = \begin{pmatrix} e^{-jkr_{11}} & e^{-jkr_{12}} \\ e^{-jkr_{21}} & e^{-jkr_{22}} \end{pmatrix}$$

where  $k = \omega \sqrt{\mu_0 \epsilon_0}$ .

The capacity is obtained as:

$$\text{if } d = .5 \rightarrow \lambda_1 = 2.0, \lambda_2 = 0 \rightarrow C_{2 \times 2} = \sum_{i=1}^2 \log_2 \left( 1 + \frac{\gamma}{2} \lambda_i \right) = 7.6 \quad \text{bps / Hz}$$

$$\text{if } d = 10 \rightarrow \lambda_1 = 1.41, \lambda_2 = .6 \rightarrow C_{2 \times 2} = \sum_{i=1}^2 \log_2 \left( 1 + \frac{\gamma}{2} \lambda_i \right) = 12.95 \quad \text{bps / Hz}$$



**Case III: MIMO Capacity with Single Scattering**

Similarly, as shown in Figure 2.3(b), by calculating  $\mathbf{H}$  and using equation (2.15), the capacity is obtained as:

$$\text{if } d = .5 \rightarrow \lambda_1 = 2.14, \lambda_2 = .2 \rightarrow C_{2 \times 2} = \sum_{i=1}^2 \log_2 \left( 1 + \frac{\gamma}{2} \lambda_i \right) = 12.01 \text{ bps / Hz}$$

**Case IV: MIMO Capacity in a Rich Scattering Environment**

By using equation (2.18) and assuming a scenario of rich scattering, the capacity is obtained as 15.2 bps/Hz.

## 2.4 MIMO Design Advantages

MIMO systems can be designed either to provide maximal diversity to increase transmission reliability or to achieve maximal multiplexing gain to support high data rates [8]. Equation (2.15) shows that the channel capacity of a MIMO system can be much higher than that of a SISO system. This performance of a MIMO system is quantified with spatial multiplexing gain. On the other hand, if the signal copies are transmitted from multiple antennas or received at more than one antenna, the multiple antenna systems can provide a gain that can improve reliability of a wireless link. This gain is called diversity gain.

Furthermore, MIMO systems can be used to simultaneously provide both diversity and multiplexing gain. However, there is a fundamental tradeoff between them, either in large SNR values [9] or finite SNR values [11].

### 2.4.1 Space-Time Codes for Diversity

In this design, the signal copies are transmitted from multiple antennas or received at more than one antenna in space-time multi-antenna systems. The average symbol error probability of a MIMO communications system for maximum likelihood (ML) detection is has an upper boundary in high SNR values as [4]:

$$p_e \leq \overline{N}_e \left( \frac{\gamma d_{\min}}{4M} \right)^{-M} \quad (2.22)$$

where  $\overline{N}_e$  is the number of nearest neighbors in a scalar constellation,  $d_{\min}$  is the minimum distance of separation of the scalar constellation, and  $M = \min\{M_R, M_T\}$ .

As can be seen in Figure 2.4, increasing the number of antennas increases the slope of the bit error rate (BER) curves and improves the reliability of wireless communications. Two general techniques to generate the space-time codes for

diversity are space-time block codes and space-time trellis codes [4], [7]. Although the space-time trellis codes were introduced earlier [12], the space-time block codes have been the preferred coding techniques in practice, due to the ease of their implementation.

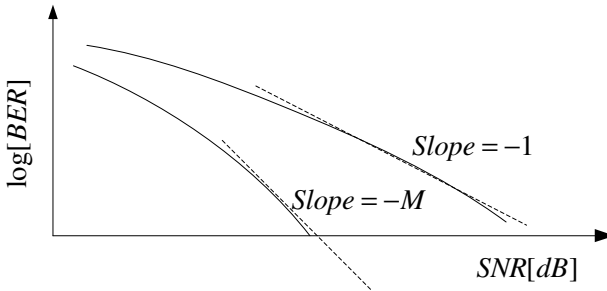


**Fig. 2.4** Space-time diversity gain in MIMO systems

■ **Example 2.3:** Alamouti Space-Time Coding

The Alamouti code is an orthogonal space-time block code (O-STBC). It is implemented by using two antennas at the transmitter and an arbitrary number of the antennas at the receiver [10]. The code words for multiple antennas are written as:

$$\mathbf{X} = \frac{1}{\sqrt{2}} \begin{pmatrix} \chi_1 & -\chi_2^* \\ \chi_2 & \chi_1^* \end{pmatrix} \quad (2.23)$$

The Alamouti transmitter is shown in Figure 2.5. The Alamouti code has a spatial multiplexing rate equal to one, as two symbols are transmitted over two symbol durations. The performance of the Alamouti code is presented in Figure 2.6.

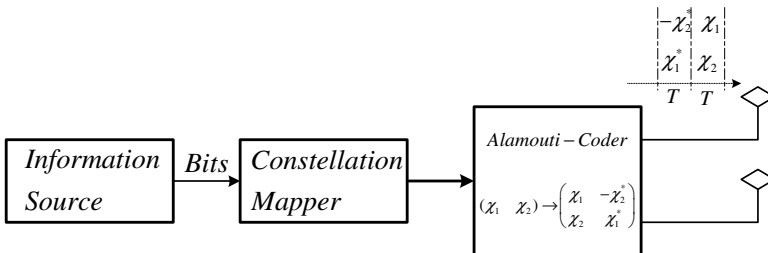


**Fig. 2.5** The Alamouti space-time coding

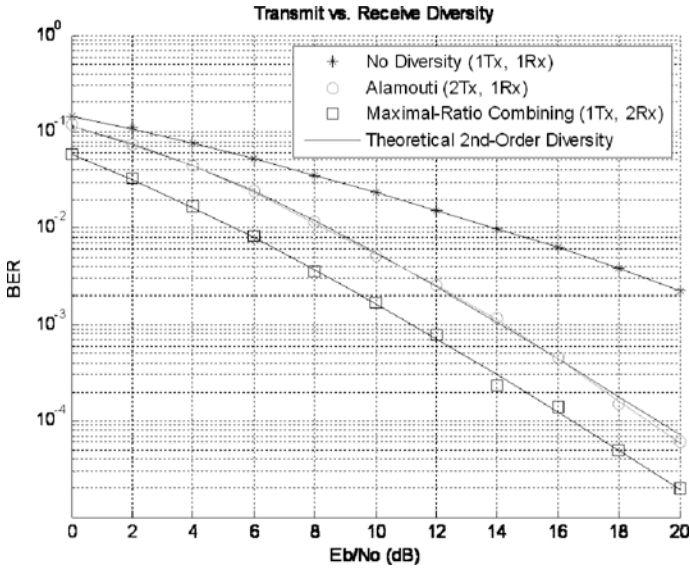


**Fig. 2.6** The performance of the Alamouti space-time code with different numbers of antennas at the receiver

### 2.4.2 Spatial Multiplexing

In the layered space-time codes for spatial multiplexing, the sequence of information bits is divided into certain sets of substreams. The substream where the signal processing is conducted is referred as a layer. Hence, this is known as the layer space-time (LAST) technique. As shown in Figure 2.7,  $M_T$  independent substreams are transmitted through  $M_T$  antennas. In this technique, the number of receiving antennas must be equal to or larger than the number of transmitting antennas [7].

The process of dividing the sequence of information into substreams is done by a demultiplexer. The demultiplexing process may be applied to bits or symbols. Hence, the encoding can be realized in three different ways according to the demultiplexer position in the transmitter chain and the direction of the layer [1]. These encoding processes are referred to as horizontal, vertical and diagonal encoding. The different encoding techniques are shown in Figure 2. 8.

In horizontal encoding, the data bits are demultiplexed into  $M_T$  substreams that are independently encoded, interleaved and modulated. On the other hand, in the vertical realization, the data stream is encoded, interleaved and modulated; and, the resulting symbols are then demultiplexed into  $M_T$  substreams. The process to realize the diagonal spatial multiplexing is similar to horizontal encoding with the only difference being that, after the final stage, the frames of symbols undergo a stream interleaver, which rotates the transmitted frames [7], [8].

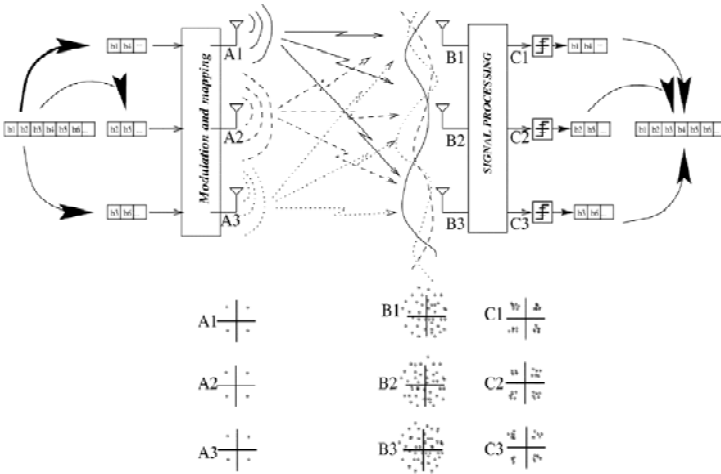


**Fig. 2.7** Spatial multiplexing with three antennas at the transmitter and three antennas at the receiver [8]

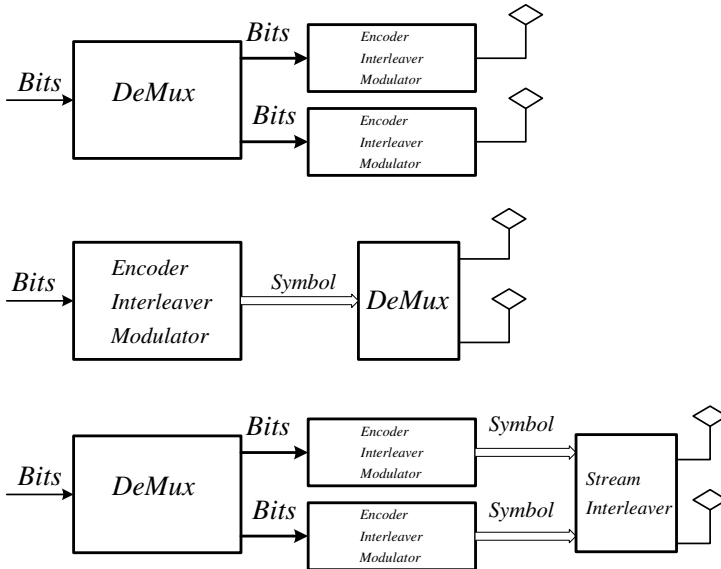


**Fig. 2.8** Spatial multiplexing encoding: a) horizontal encoding, b) vertical encoding, c) diagonal encoding

### 2.4.3 Diversity-Multiplexing Tradeoff

The channel capacity of a MIMO system can be considerably higher than that of a SISO system using layered space-time coding. This performance of a MIMO channel provides spatial multiplexing gain. On the other hand, MIMO systems can improve the reliability of a wireless link; and, this performance provides diversity gain. Traditionally, MIMO systems have been designed to extract either maximal diversity or spatial multiplexing gain.

MIMO systems, however, can provide both diversity gain and multiplexing gain. In [9], an optimal tradeoff curve between the asymptotic diversity and the multiplexing gain has been derived at infinite SNR. The diversity gain is obtained as:

$$d = \lim_{\rho \rightarrow \infty} - \frac{\log P_{out}}{\log \rho} \quad (2.24)$$

The spatial multiplexing gain is defined as:

$$r = \lim_{\rho \rightarrow \infty} \frac{R}{\log \rho} \quad (2.25)$$

where  $d$  is the diversity gain,  $r$  is the multiplexing gain,  $P_{out}$  is the outage probability,  $R$  is the data rate in bps/Hz, and  $\rho$  is average SNR per antenna. It has been shown that the most famous space-time coding schemes, such as space-time block code (STBC) and Bell layered space-time (BLAST), are not optimal with respect to the diversity-multiplexing tradeoff (DMT) criteria. The asymptotic diversity multiplexing tradeoff and the finite SNR diversity multiplexing tradeoff for MISO/SIMO and MIMO are presented in Figures 2.9 and 2.10 [14].

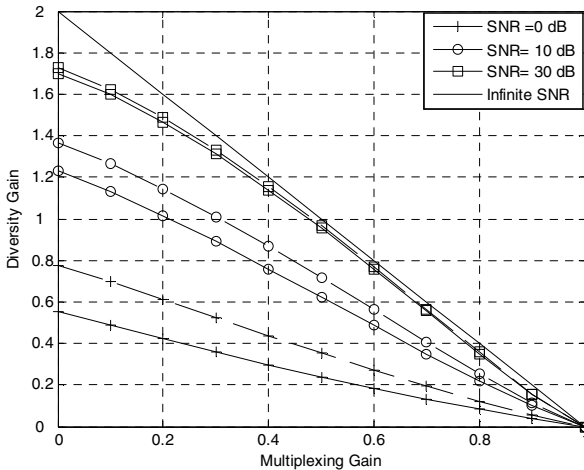


**Fig. 2.9** Diversity-multiplexing tradeoff curve for SIMO (dashed lines) and MISO (solid lines) using two antennas

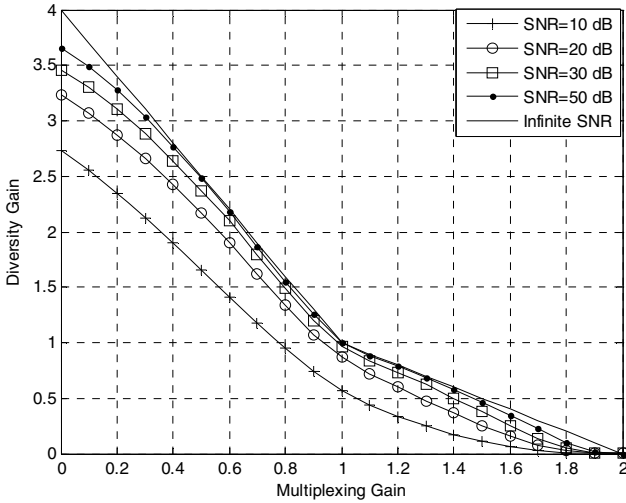


**Fig. 2.10** Diversity-multiplexing tradeoff curve for MIMO (2 X 2)

## 2.5 MIMO Channel Models

There are different classifications for MIMO channels [2], [16]. As shown in Table 2.1, a classification based on the modeling approach divides the models into physical models and analytical models. Physical channel models characterize a channel on the basis of electromagnetic wave propagation. They explicitly model wave propagation parameters, such as the complex amplitude and delay. More sophisticated models also incorporate polarization and time variation. Physical models are independent of antenna configurations (antenna pattern, number of antennas, array geometry, polarization, mutual coupling) and system bandwidth [16].

Physical MIMO channel models can further be split into deterministic models, geometry-based stochastic models, and non-geometric stochastic models. Deterministic models characterize the physical propagation parameters in a completely deterministic manner, e.g. ray tracing. Using geometry-based stochastic channel models, the impulse response is characterized by the laws of wave propagation applied to specific transmitters (Tx) and receivers (Rx) and scatterer geometries, which are chosen in a stochastic (random) manner. In contrast, non-geometric stochastic models describe and determine physical parameters in a completely stochastic way by prescribing underlying probability distribution functions without assuming an underlying geometry [17].

In contrast to physical models, analytical channel models characterize the impulse response of the channel between the individual transmitting and receiving antennas in a mathematical/analytical way without explicitly accounting for wave

propagation. The individual impulse responses are subsumed in a MIMO channel matrix. Analytical models are very popular for synthesizing MIMO matrices in the context of system and algorithm development and verification.

**Table 2.1** MIMO Channel Modeling Classification

Physical Models	Analytical Models
<i>Deterministic, e.g. ray tracing</i>	<i>Correlation based</i>
<i>Geometry-based Stochastic</i>	<i>Propagation motivated</i>
<i>Non-geometrical stochastic, e.g. Saleh-Valenzuela's method [17], [19]</i>	

Analytical models can be further subdivided into correlation-based models and propagation-motivated models. Correlation-based models characterize the MIMO channel matrix statistically, in terms of the correlations between the matrix entries. The propagation-motivated models characterize the channel matrix via propagation parameters.

On the other hand, empirical methods can be extracted from analytical and physical models based on experimental results [18], [19]. They either generalize the tap-delay line concept to include the directional domains or use a combination of tap-delay lines and geometry-based models with prescribed parameters. These models are very useful for simulation purposes. They also constitute the background of many standardized channel models, such as 3GPP, COST 259, COST 273, IEEE 802.16a, IEEE 802.16e, and IEEE 802.11n.

### 2.5.1 Stanford University Interim Channel Models

In this section, the Stanford University Interim (SUI) channel models of MIMO systems are briefly discussed [2], [19], [20], [24]. SUI channel models have been developed for fixed wireless access networks at 2.5 GHz [16]. The general architecture of the SUI model is presented in Figure 2.11.

The input-mixing matrix models transmitter antenna correlations, and the output-mixing matrix presents the receiver antenna correlations. The SUI channel models basically use a three tap-delay line to model the multipath fading [4], [20]. Antennas are assumed to be omnidirectional on both the transmitting and receiving sides. The Doppler spectrum is assumed to be given by:

$$S(v) = 1 - 1.720\left(\frac{v}{v_m}\right)^2 + 0.785\left(\frac{v}{v_m}\right)^4 \quad v \leq v_m \quad (2.26)$$

where  $v_m$  is the maximum Doppler frequency.

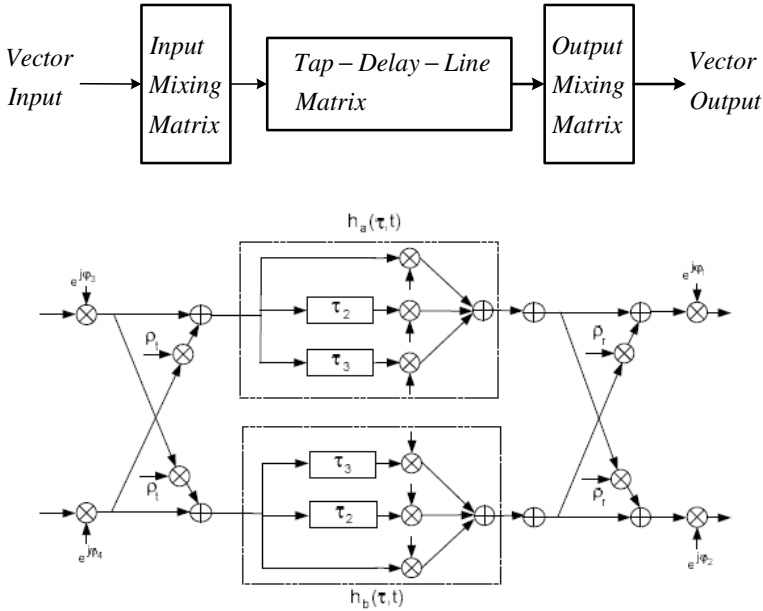


**Fig. 2.11** Schematic of a SUI channel [4]

The models describe six types of channels, numbered from 1 to 6 [21]. As an example, the parameters of SUI channel 1 are presented in Table 2.2.

**Table 2.2** The channel parameters for SUI-1 model

SUI-1 Model	Tap 1	Tap 2	Tap 3
Delay [microsec]	0.0	0.4	0.9
Power [dB]	0	-15	-20
99% K-factor	4	0	0
Doppler Frequency [Hz]	0.4	0.3	0.5
Envelope Antenna Correlation	0.7	0.7	0.7

■ **Example 2.4: IEEE 802.16d/e Models**

These models are intended for macro-cellular fixed wireless access [24]. The targeted scenario is as follows:

- The cell size is less than 10 km in radius,
- The user’s antenna is installed under the eaves or on the rooftop, and
- The base station height is 15 to 40 m.



In fact, the IEEE 802.16 model is an improved version of the SUI channel models and is valid for both omnidirectional and directional antennas. The use of directional antennas cause the global K-factor to increase, while the delay spread decreases. As an example, Table 2.3 indicates how SUI channel 4 is modified when the terminal antenna has a 30-degree beamwidth. An additional feature of the IEEE 802.16 standard is a model for the narrowband Ricean K-factor:

$$K = K_0 F_s F_h F_b R^\gamma u \quad (2.26)$$

where  $F_s$  is a seasonal factor,  $F_s = 1.0$  in summer (leaves) and 2.5 in winter (no leaves);  $F_h$  is the receiving antenna height factor,  $F_h = 0.46(h/3)$  ( $h$  is the receiving antenna height in meters);  $F_b$  is the beamwidth factor,  $F_b = -0.62(b/17)$  ( $b$  in degrees);  $K_0$  and  $\gamma$  are regression coefficients,  $K_0 = 10$  and  $\gamma = -0.5$ ; and,  $u$  is a log-normal variable, i.e.  $10\log_{10}(u)$  is a zero-mean normal variable with a standard deviation of 8 dB.

**Table 2.3** IEEE 802.16 Model

IEEE 802.16 Model	Tap 1	Tap 2	Tap 3
Delay [microsec]	0.0	1.5	4
Power [dB]	0	-10	-20
99% K-factor	1	0	0
Doppler Frequency [Hz]	0.2	0.15	0.25
Envelope Antenna Correlation	0.3	0.3	0.3

## References

- [1] Carlson, A.B., Crilly, P.B., Rutledge, J.C.: Communication Systems: An Introduction to Signal and Noise in Electrical Communications, 4th edn. McGraw Hill (2001)
- [2] Oestges, C., Clerckx, B.: MIMO Wireless Communications: From Real World Propagation to Space Time Code Design. Academic Press (2007)
- [3] Pahlavan, K., Levesque, A.: Wireless Information Networks, 2nd edn. John Wiley and Sons (2005)
- [4] Paulraj, A., Nabar, R., Gore, D.: Introduction to Space-Time Wireless Communications. Cambridge University Press (2003)
- [5] Lee, W.C.Y.: Estimation of channel capacity in Rayleigh fading environment. IEEE Transactions on Vehicular Technology 39(3), 187–189 (1990)
- [6] Mohammadi, A., Kumar, S.: Characterization of Adaptive Modulators in Fixed Wireless ATM Networks. IEEE/KICS Journal of Communications and Networks 6(2), 123–132 (2004)
- [7] Tsoulos, G.: MIMO System Technology for Wireless Communications. CRC Press (2006)
- [8] Gesbert, D., Shafi, M., Shiu, D., Smith, P.J., Naguib, A.: From Theory to Practice: An Overview of MIMO Space–Time Coded Wireless Systems. IEEE Journal on Selected Areas in Communications 21(3), 281–302 (2003)

- [9] Zheng, L., Tse, D.N.C.: Diversity and multiplexing: a fundamental tradeoff in multiple antenna channels. *IEEE Transactions on Information Theory* 49, 1073–1096 (2003)
- [10] Alamouti, S.M.: A simple transmit diversity technique for wireless communications. *IEEE Journal on Selected Areas in Communications* 16(10), 1451–1458 (1998)
- [11] Ebrahimzad, H., Mohammadi, A.: On Diversity-Multiplexing Tradeoff in MIMO channel at Finite SNR. *IEICE Transactions on Fundamentals of Electronics, Communications and Computer Sciences* E93-A(11), 2057–2064 (2010)
- [12] Tarokh, V., Seshadri, N., Calderbank, A.R.: Space-time Codes for High Data Rate Wireless Communication: Performance Criterion and Code Construction. *IEEE Transactions on Information Theory* 44(2), 744–765 (1998)
- [13] Gershman, A.B., Sidiropoulos, N.D.: *Space-Time Processing for MIMO Communications*. Wiley (2005)
- [14] Ebrahimzad, H., Mohammadi, A.: Diversity-Multiplexing Tradeoff in MIMO Systems with Finite SNR. In: *European Conference on Wireless Technology, Munich*, pp. 146–149 (October 2007)
- [15] Papoulis, A., Pillai, S.U.: *Random Variable Variables and Stochastic Process*, 4th edn. McGraw Hill (2002)
- [16] Almers, P., Bonek, E., Burr, A., Czink, N., Debbah, M., Degli-Esposti, V., Hofstetter, H., Kyosti, P., Laurenson, D., Matz, G., Molisch, A.F., Oestges, C., Ozcelik, H.: Survey of Channel and Radio Propagation Models for Wireless MIMO Systems. *EURASIP Journal on Wireless Communications and Networking* 2007, article ID 19070, 19 pages (2007)
- [17] Saleh, A.M., Valenzuela, R.A.: A statistical model for indoor multipath propagation. *Journal on Selected Areas in Communications* 5(2), 128–137 (1987)
- [18] Rappaport, T.S.: *Wireless Communications: Principles and Practice*, 2nd edn. Prentice Hall (2002)
- [19] Wallace, J.W., Jensen, M.A.: Modeling the indoor MIMO wireless channel. *IEEE Transactions on Antennas and Propagation* 50(5), 591–599 (2002)
- [20] Baum, D.S., Gore, D.A., Nabar, R.U., Panchanathan, S., Hari, K.V.S., Erceg, V., Paulraj, A.J.: Measurement and characterization of broadband MIMO fixed wireless channels at 2.5 GHz. In: *Proceedings of the International Conference on Personal Wireless Communications (ICPWC 2000)*, India (December 2000)
- [21] Erceg, V., et al.: IEEE p802.16 – channel models for fixed wireless applications (iee802.16.3c-01/29r4) (2001)
- [22] Correia, L.M.: *COST 259 – Wireless flexible personalized communications*. Wiley, London (2001)
- [23] Correia, L.M.: *COST 273 – Towards mobile broadband multimedia networks*. Elsevier, London (2006)
- [24] IEEE P802.16 e /D12, IEEE Standard for Local and metropolitan area networks Part 16: Air Interface for Fixed and Mobile Broadband Wireless Access Systems Amendment for Physical and Medium Access Control Layers for Combined Fixed and Mobile Operation in Licensed Bands (October 2005)
- [25] Flaviis, F.D., Jofre, L., Romeu, J., Grau, A.: *Multiantenna Systems for MIMO Communications*. Morgan & Craypool Publishers (2008)